IOP Conf. Series: Materials Science and Engineering **418** (2018) 012039 doi:10.1088/1757-899X/418/1/012039

Development of a New Index to Depict the Total Forming Capacity of Sheet Metals

L Huang and M F Shi

United States Steel Corporation, 5850 New King Court, Troy, MI 48098, USA

lhuang@uss.com

Abstract. The forming limit curve (FLC) has been used to represent the stretchability of sheet metal under various forming modes. However, the formability window in stamping depends not only on the material's forming limit, but also on its strain distribution ability. In the present work, a total forming capacity (TFC) index is introduced to describe the global formability of sheet metals, which accounts for the contributions of both forming limit and strain distribution ability in the material during forming. Essentially, this index is constructed by integrating the instantaneous n-value from zero to the effective strain limit of the material. The usefulness of this new index is demonstrated through a comparison of the overall global formability between a cold-rolled (CR) 590DP steel and a CR980GEN3 steel via a dome test coupled with digital image correlation (DIC). Contradicting of its lower forming limit, the 980GEN3 can be formed to a higher limiting dome height (LDH) than the 590DP under a near plane strain condition. This superior overall global formability of 980GEN3 is attributed to its capability to dissipate strain uniformly during forming, resulting in lower strain gradient and delayed strain concentration. While revealing the limitation of using the FLC alone, findings in this study evince the strength and effectiveness of this new index in assessing the overall global formability of sheet metals. The higher index is successfully correlated to the higher LDH of the 980GEN3. Further, the TFC concept is applied to evaluate the global formability of a multitude of high strength steels at different thicknesses. An explicit relationship is established between the calculated index and experimental LDH results. The development and application of the TFC indices promise a straightforward way to assess the overall global formability of a material. It also serves as a more precise yet simple tool for material comparisons and selections.

1. Introduction

Sheet metals constitute the most important family of materials employed in the automotive industry [1, 2]. To successfully form a 2-dimentional (2D) sheet metal to a 3-dimentioanal (3D) automotive part (i.e., B-pillar, door inner, crossmember, roof rail, etc.), the understanding of its formability is critical [2, 3]. The past decades have witnessed soaring development of advanced high strength steels (AHSS) and other new metallic/non-metallic sheet materials. The growing applications of these new materials in recent and future body-in-white (BIW) designs have placed new emphasis to utilize the maximum forming capacity of these materials during stamping or other forming processes [1].

Conventionally, the global formability of sheet metals has been evaluated using forming limit curves (FLCs) to describe the limiting strains at the onset of localized necking (through thickness thinning) in a sheet material under different strain conditions [4-8]. Other mechanical property

parameters such as total elongation (TE) and uniform elongation (UE) are also frequently adopted as simple comparators to distinguish the formability of materials [1, 8]. Meanwhile, the importance of enabling uniform strain distribution in sheet metal forming has been recognized [9-12]. In this regard, the work hardening exponent, commonly known as the n-value, was often referred to as an intrinsic parameter to measure the strain distribution competence of the material. Previous analyses on the instantaneous n-value as a function of strain were found helpful to evaluate the formability of sheet materials [9, 10].

It is generally acknowledged that the formability window of a sheet material in stamping depends not only on the material's forming limit but also on its strain distribution ability. A recent report from Zhang et al., which was conducted independently from the present work, accentuated the necessity to consider both aspects of the global formability [12]. They have evaluated the formability of the QP980 and three DP980 steels and found inconsistent results in the formability comparisons when using different parameters. Two indices were proposed in their work to respectively describe the global formability (average strain, ε_A) and uniform deformation capability (the extent of non-uniform deformation, H). The determination of these two indices requires mathematical manipulations of temporal and spatial strain data based on digital image correlation (DIC) analysis. Despite recent advances, there remains the absence of a single parameter to describe the overall forming capacity of a sheet material. In this work, a novel index, named total forming capacity (TFC) index, is proposed to account for both forming limits and strain distribution ability of the material for formability evaluations and material selections. The proposed index can be conveniently determined using the stress-strain curve and the FLC, which are usually readily available from material development and/or qualification work. The usefulness of the new index is first demonstrated through a comparison on the global formability between a cold-rolled (CR) 590 dual phase (DP) steel and a CR 980 third generation (GEN3) steel. Further, its effectiveness is validated with a multitude of high strength steel grades of different thicknesses.

2. Design of the TFC Index

2.1. Definition

The TFC index is proposed as described in Equation (1):

$$\mathrm{TFC} = \int_0^{\varepsilon_{\mathrm{limit}}} n_{\mathrm{inst}}(\varepsilon)\mathrm{d}\varepsilon \times 100 \quad (1)$$

where $\varepsilon_{\mathrm{limit}}$ is the limiting strain at failure that is defined to be the effective strain ($\varepsilon_{\mathrm{eff}}$) at the forming limit from the path independent FLC [13]; $n_{\mathrm{inst}}(\varepsilon)$ is the instantaneous n-value as a function of true plastic strain to reflect the material's strain distribution capability. Equation (1) can also be applied to shear conditions by using the equivalent failure strain in shear as $\varepsilon_{\mathrm{limit}}$.

As schematically demonstrated in Figure 1, this TFC index is constructed by integrating the instantaneous n-value from zero to the effective limit strain of the material. In other words, the value of the TFC index for the material equals to the area underneath the instantaneous n-value curve up to the effective forming limit strain under a specified strain condition. A scale factor of 100 is incorporated in Equation (1) to eliminate excessive zeros after the decimal point for the clarity of data presentation. Essentially, a TFC describes the material's overall capability to dissipate strain within itself before reaching strain limits at localized necking. The physical meaning of a TFC index is analogous to a strain energy threshold that can be reached during deformation prior to failure.

2.2. Assumptions

The following assumptions have been made to simplify the calculation of the TFC in this study, in order to facilitate the investigation on the initial feasibility of using this new index for formability characterizations:

1) The materials are assumed to obey the von Mises yield criterion. The effective strain is calculated using Equation (2).

$$\varepsilon_{eff}= \frac{\sqrt{2}}{3}\times\sqrt{(\varepsilon_1-\varepsilon_1)^2+(\varepsilon_1-\varepsilon_3)^2+(\varepsilon_2-\varepsilon_3)^2} \quad (2)$$

This assumption is considered suitable for most of the materials studied in our current work, which are high strength steels with average r values of approximately 1. An anisotropy yield criterion should be used for those materials with strong anisotropy behaviors.

2) Based on the n-value definition, the instantaneous n-value can be calculated using the following equation:

$$n_{inst}(\varepsilon)= \frac{d\ln(\sigma)}{d\ln(\varepsilon)} \quad (3)$$

3) The effective true stress-strain curve of the material is identical under different strain paths and the true stress-strain curve obtained from a tension test is to be applied. In other words, the working hardening behavior (n-value) derived from the effective stress and strain data is the same for all strain paths including nonlinear strain paths (NLSP).
4) Before reaching UE, $n_{inst}(\varepsilon)$ can be calculated using Equation (3) based on the tension test data. However, extrapolation of $n_{inst}(\varepsilon)$ beyond UE is necessary, since the n-value calculation is invalid using tensile data beyond UE. It is supposed that the working hardening behavior of the material after UE maintains the same as that at UE and the n-value beyond UE remains as a constant that equals to the terminal n-value (n_{term}). For those materials demonstrating different work hardening behaviors beyond UE, other assumptions may be used to account for the true behavior of the material.
5) A linear strain path is assumed for the FLC (limit strains) and in the subsequent TFC calculation.

Major assumptions stated above are visualized in Figure 2. It is emphasized that the above assumptions are not intrinsic to a TFC index. Complexity in the TFC calculation can be built up by removing one or more assumptions to improve the accuracy of the index calculation. This initial proposal is to check the effectiveness of the index in measuring the total forming capacity.

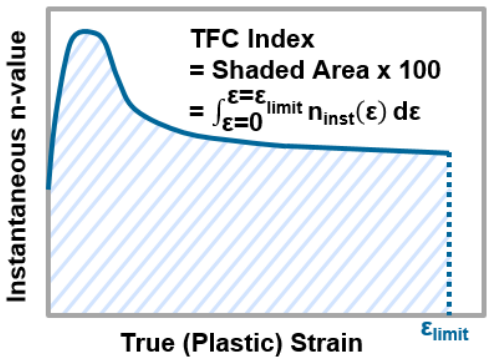

Figure 1. Schematic demonstration of the definition of a TFC index.

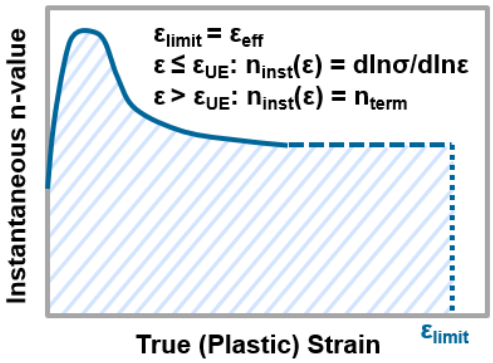

Figure 2. Assumptions applied to the TFC calculations in this work.

3. Materials and Experimental Methods

As a proof-of-concept, a series of experiments were conducted using various high strength steels with ultimate tensile strengths (UTS) ranging from 440 MPa to 1180 MPa, as listed in Table 1.

Tension tests were conducted in the transverse direction for all test materials following ASTM E08 standard [14]. Typical tensile properties of the materials are presented in Table 1. The engineering stress-strain curve from the tension test was converted to true stress-strain up to UE. Subsequently, the instantaneous n-value curve as a function of true plastic strain can be generated using Equation (3).

The Nakazima dome test following ASTM E2218 standard [15] was used to evaluate the overall global formability of the materials. Test specimens were machined in the transverse direction to a designed geometry to achieve a near plane strain condition. Example specimens before and after test

are shown in Figure 3a. A 3D DIC system was utilized to record the forming process at an acquisition rate of 15 frames per second. DIC images were subjected to post-processing at a virtual gauge length of 2.75 mm to obtain spatial and temporal strain data (e.g., strain evolution and distribution) on the top surface of the specimen (Figure 3b). Detailed descriptions of the test configuration and procedure can be found in our previous publications [16, 17]. True major (ε_1) and true minor (ε_2) strains at the forming limit of the material were determined using the algorithm laid out in the ISO 12004-2 standard [18]. The thickness strain limit (ε_3) was calculated by assuming volume constancy [$\varepsilon_3 = -(\varepsilon_1 + \varepsilon_2)$]. The dome height at the time point when the thickness strain limit was reached was considered the limiting dome height (LDH) of the material.

Table 1. Test materials and their typical mechanical properties in transverse direction.

Grade	Material	t (mm)	YS (MPa)	UTS (MPa)	UE (%)	TE (%)	n_{term}
440	CR440W	1.4	335	466	17.7	31.2	0.163
590	CR590DP	1.4	378	643	14.0	22.9	0.131
780	EG780TRIP	1.4	524	838	19.8	25.6	0.181
780	GA780TRIP	1.2	488	814	13.9	18.6	0.130
780	GI780DP	1.2	542	876	10.8	15.7	0.102
980	CR980GEN3	2.3	597	999	17.1	23.1	0.158
980	CR980GEN3	1.8	598	997	16.4	21.6	0.152
980	CR980GEN3	1.4	640	1005	16.4	21.7	0.152
980	CR980GEN3	0.8	633	1027	15.4	21.3	0.143
980	CR980TBF	2.3	950	1091	7.5	12.5	0.072
980	CR980TBF	1.4	868	1010	7.0	12.0	0.067
980	CR980TBF	1	880	1061	8.4	12.4	0.080
1180	CR1180SHF	1.6	930	1201	9.0	13.2	0.080
1180	CR1180SHF	1.2	933	1217	8.3	12.9	0.080
1180	CR1180SHF	1	938	1205	8.3	12.6	0.086

t: thickness; YS: yield strength; UTS: ultimate tensile strength; UE: uniform elongation; TE: total elongation; n_{term}: terminal n-value; CR: cold-rolled (bare); EG: electrogalvanized; GA: hot-dip galvannealed; GI: hot-dip galvanized

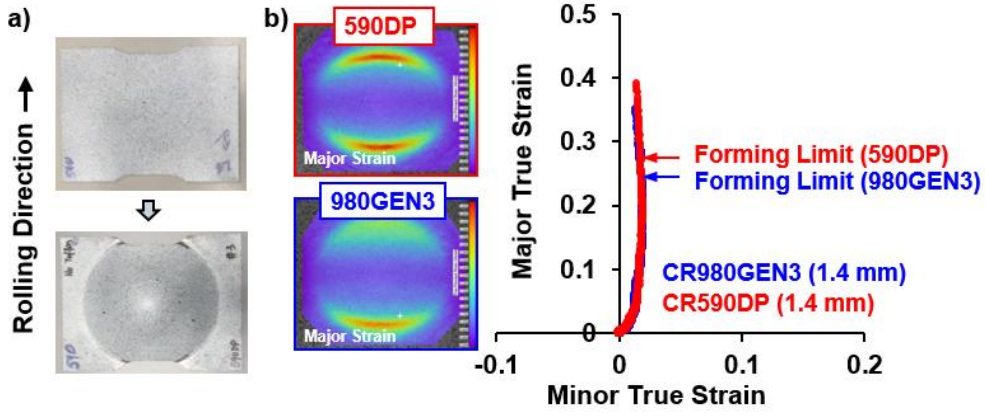

Figure 3. Formability tests coupled with DIC: a) example test specimens of the CR590DP before (top) and after (bottom) Nakazima dome test; b) DIC data showing strain contours at the last frame prior to fracture, strain histories and forming limits of the CR980GEN3 and the CR590DP.

4. Results and Discussion

4.1. Case study: CR590DP and CR980GEN3

To excise the proposed TFC index, a case study was conducted to assess and compare the formability of the CR590DP and the CR980GEN3 steels of 1.4 mm thickness.

As discussed earlier, many mechanical properties have been cited to characterize the formability of a material, amongst which the FLC, the TE, the UE and the n-value are most frequently used. The formability comparisons between the CR590DP and the CR980GEN3 using these properties yield contradicting results. Based on the FLCs in Figure 4 and results in Table 1, the CR590DP is found to show higher FLC and TE than the CR980GEN, which would usually be interpreted as better formability for the CR590DP. However, the UE and n_{term} for the CR980GEN3 are higher than the CR590DP based on the stress-strain curves in Figure 5 and mechanical properties listed in Table 1, which indicates a superior strain distribution capability of the CR980GEN3.

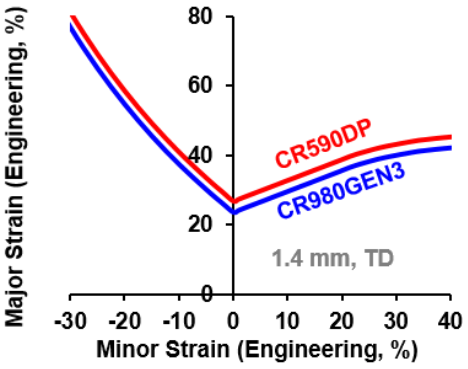

Figure 4. FLCs of the CR590DP and the CR980GEN3 based on dome tests.

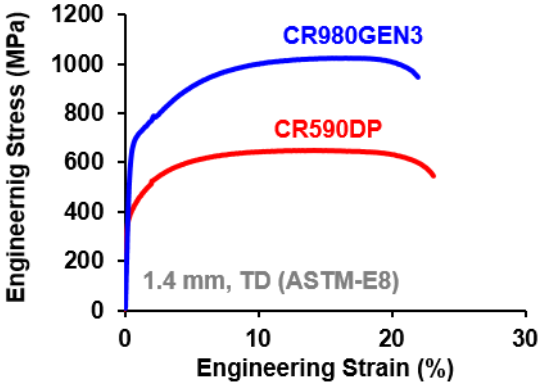

Figure 5. Engineering stress-strain curves of the CR590DP and the CR980GEN3.

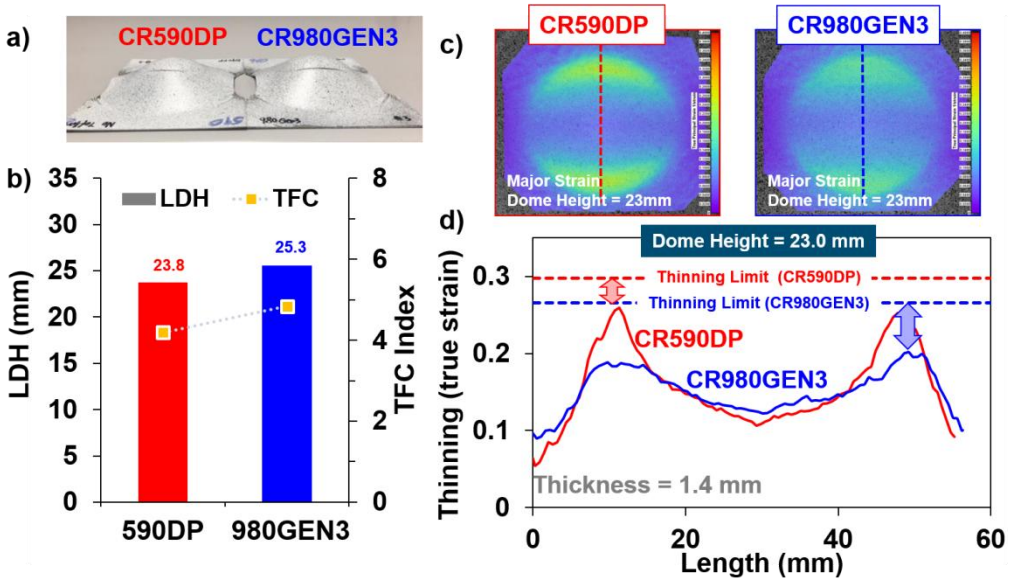

Figure 6. Comparisons on the formability of the CR590DP and the CR980GEN3: a) samples after test; b) LDH and TFC index comparison; c) strain distribution contours at dome height of 23 mm; and d) strain distribution profiles along the middle lines indicated in c), arrows illustrate the sizes of the formability windows.

LDH tests were adopted for a direct comparison in the global formability between the two materials, and the results are illustrated in Figures 6a and b. Opposing to its lower forming limit, the CR980GEN3 can be formed to a higher LDH under the near plane strain condition than the CR590DP.

The superior global formability of the CR980GEN3 to the CR590DP is largely attributed to its capability to dissipate strain uniformly during forming. This is proved by the DIC analysis shown in Figures 6c and d. At the same dome height of 23 mm, the strain gradient in the CR980GEN3 is much smaller than in the CR980GEN3, leading to a larger formability window despite its lower thinning limit.

In this case study, FLC and TE failed to predict the overall global formability advantage of the CR980GEN3. UE and n-value are seemingly more appropriate criteria, however, may result in overestimation of the formability differences between the two materials, since the strain limits are not accounted for. The TFC index was introduced to solve this conundrum. Calculation of the TFC was performed using the method sketched in Figure 2 and are plotted in Figure 6b. The higher TFC index is successfully correlated to the higher LDH of the CR980GEN3, preliminarily showing the effectiveness of the TFC index to characterize and compare global formability of materials. The ability of the TFC index to reflect the extent of formability difference between the two materials appears satisfactory. The effectiveness of the TFC index will be further discussed in the following sections.

4.2. Additional applications of TFC index

The general applicability and scalability of the proposed TFC index were explored with 15 high strength steels of a spectrum of grades (UTS: 440 – 1180 MPa) and thicknesses (0.8 – 2.3 mm) as tabulated in Table 1. The results are summarized in Figure 7. A different strain path was also examined for the 1.4 mm thick CR980GEN3 denoted with the asterisk in Figure 7.

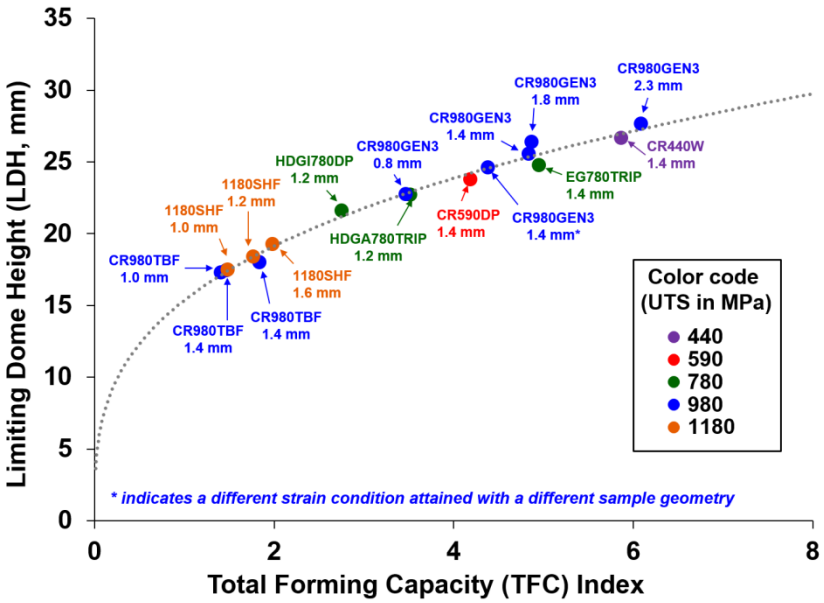

Figure 7. LDH as a function of TFC of high strength steels at different strength levels, different thicknesses and under different strain conditions. A power law relationship is established between LDH and TFC.

An explicit relationship is established between the calculated TFC index and the experimental LDH at the near plane strain conditions, which is evinced in Figure 7. Statistically, this relationship is best depicted by a power law with an R^2 value of 0.989:

$$LDH = 15.4 \times TFC^{0.32} \quad (4)$$

or $$TFC=\frac{\ln(LDH)-2.73}{0.32} \quad (5)$$

The power law relationship between LDH results and TFC indices is fundamentally meaningful, as the LDH is 0 when the TFC equals to 0. On an additional note, a linear regression in the form of $LDH=2.217\times TFC+14.54$ can also provide acceptable fitting results (R^2 = 0.9753). However, it is rejected for not being physically sound to correlate 0 forming capacity with a large LDH.

Some deviations from the power law can be identified in Figure 7, which could be inherent to the assumptions made in section 2.2. Moreover, the accuracy of LDH and the subsequent relationship determined above is dependent on the accuracy in the forming limit determination. In this work, the more conservative DIC data processing method following ISO12004-02 standard was utilized [16], which may systematically offset the calculated TFC indices to lower values. The model will be further improved to optimize the coefficients in Equation (4) in future work.

4.3. TFC Curve, TFC_0, and TFC_{UT}

The definition in Equation (1) implied that the TFC index is dependent on material thickness and strain path. The strain path and thickness dependent features of the TFC are built in due to the use of the forming limit (FLC) in the calculation. Therefore, the TFC is not a fixed number, but rather a curve for a specific sheet material. For each data point along the FLC, an effective strain limit can be calculated with Equation (2) and volume constancy assumption, converting the typical FLC in an ε_1-ε_2 diagram to an effective FLC in an ε_{eff}-ε_2 diagram. Such conversion is shown in Figure 8a with CR980GEN3 as an example. Data points in the effective FLC (Figure 8a) coupled with the extrapolated instantaneous n-value curve can be applied to calculate corresponding TFC indices using Equation (1), which is schematically demonstrated in Figure 8b for the CR980GEN3. Subsequently, a TFC curve can be constructed and plotted in a TFC-ε_2 diagram. The TFC curves of the CR590DP and the CR980GEN3 are illustrated in Figure 8c, in comparison with their FLCs. Similar to but more precise than the FLCs, the TFC curves can be applied to give a comprehensive evaluation and comparison of a material's total capability in global forming. The example in Figure 8c displays even more global forming benefits of the CR980GEN3 than the CR590DP under uniaxial tension and biaxial stretch conditions, which are not visible in the FLC comparisons.

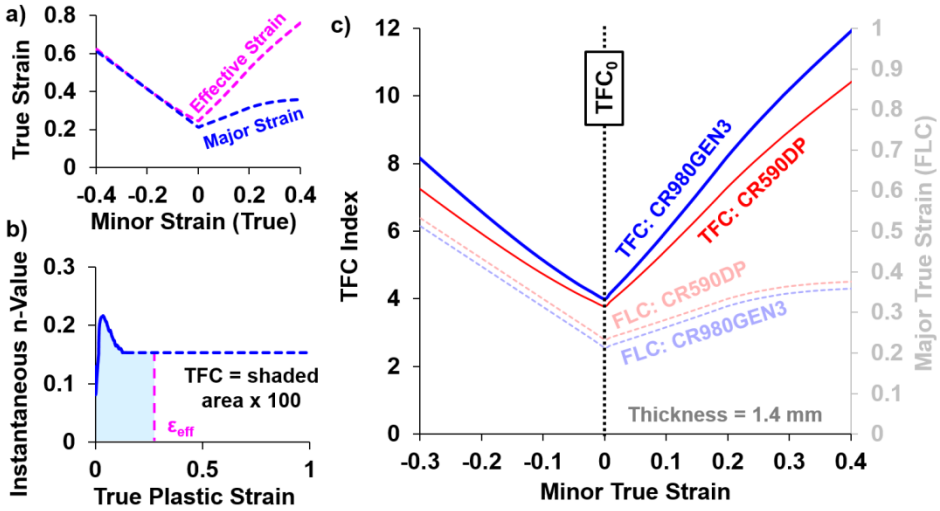

Figure 8. Calculation of a TFC curve: a) converting typical FLC (blue dashed line) to effective FLC (pink dashed line) for a 1.4 mm thick CR980GEN3; b) instantaneous n-value curve and schematic TFC construction for a 1.4 mm thick CR980GEN3; c) comparisons on the FLCs (dashed lines) and TFC curves (solid lines) of the CR590DP and the CR980GEN3.

To facilitate material comparison, the use of the TFC index under plane strain condition (TFC_0) is recommended, which is corresponding to FLC_0, as shown in Figure 8c. One example of the application of TFC_0 is shown in Figure 9 as a TFC_0-thickness diagram. The properties of three materials are plotted for demonstration purposes. This diagram can be used for an accurate and quick comparison of materials' global formability. At the same thickness (e.g., 2 mm), the higher TFC_0 values of the EG780TRIP and the CR980GEN3 than that of the CR590DP are indicative of their superior global formability. Additionally, the diagram is useful in the down-gauging feasibility evaluation. In this regard, the use of a 1.75 mm CR980GEN3 or a 1.0 mm EG780TRIP to replace the 2.0 mm thick CR590DP could be practical without any changes to the part design from the global formability point of view. If further down-gauging is desired, design modifications to the part/tool may be required for the same global formability window. It is important to reiterate that the evaluation is only valid concerning global forming. Local formability of the materials should be assessed separately.

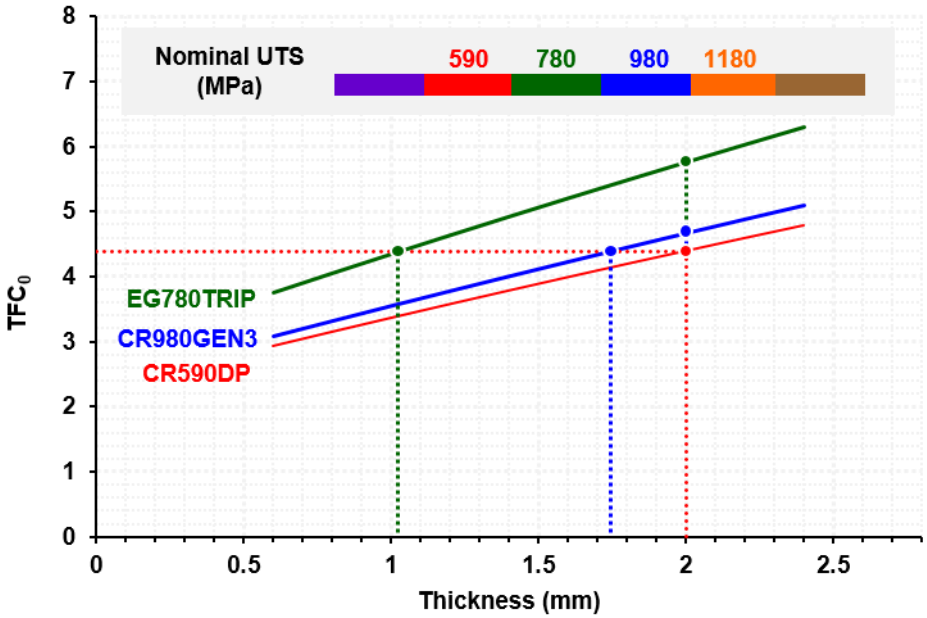

Figure 9. TFC_0-thickness diagram for global formability comparisons and down-gauging feasibility evaluation

Alternative to the TFC_0, the TFC under uniaxial tension condition (TFC_{UT}) can be another useful parameter for direct material comparisons. The benefit of using TFC_{UT} is that it can be determined solely based on tension tests. TFC_{UT} can also be used for material ranking, selection, and material replacement feasibility evaluation purposes. The determination and applications of TFC_{UT} are not elaborated in this paper, since it is essentially similar to the TFC_0.

4.4. Additional discussion and future considerations

A number of assumptions were incorporated in the TFC calculation to simplify the discussion in the present study, as listed in Section 2.2. For future development to improve the accuracy of the index and to expand its applicability to other sheet materials, additional considerations and reviews to these assumptions are necessary.

First, the precision of the instantaneous n-value curve governs the accuracy of the TFC index. Current assumption of a constant n-value beyond UE may not hold true for materials with dynamic n-value at higher true strains, such as TRIP steels or aluminum alloys. Optimization of n-value extrapolation beyond UE using different work hardening models would be helpful to certain extent.

Ideally, experimental tests (e.g., bulge test, shear test, etc.) should be performed to generate the true stress-strain curve and instantaneous n-value curve to high strains.

Second, the NLSP dependence of the TFC curve is worth emphasis. The TFC computation can be affected by the presence of NLSP in the test, which is inherent from the strain path dependence of the FLC [19] used in the calculation. With the attempt to rule out this process-dependent factor in material property comparison, the strain paths of the dome test under near plane strain deformation modes were approximated to be linear in this study. For the relative material performance evaluation purpose, the TFC calculated from the FLC with the linear strain path should be sufficient. To ensure the validity of the TFC definition in Equation (1) for the NLSP, the use of the path independent FLC [13] is required. In this case, the upper limit for the integration in Equation (1) becomes the effective limit strain corresponding to the incremental strain ratio [13]. As a result, the x-axis in Figure 8c can be replaced with the incremental strain ratio to generate a TFC vs. the incremental strain ratio diagram, so that the TFC would be independent of the nonlinear strain path. It is reiterated that the working hardening behavior is assumed to be independent of the strain path including NLSP.

In addition to the significances of considering dynamic n-value and NLSP effects in the TFC calculations, other works are on-going or proposed, including:

1) Expanding the test matrix to increase the number of data points for a more general statistical analysis covering different materials, wider range of grades, larger span of strain paths, etc..
2) Considerations of different yield criteria and material anisotropy.
3) Possible variations in work-hardening behavior and effective stress-strain curve under various deformation modes and NLSPs [20].
4) Utilization of a more accurate data analysis method to determine forming limits [17].

5. Conclusions

In this work, a new concept named TFC index is developed to evaluate the global formability of sheet materials. Contributions from both forming limit and strain distribution ability to the material's global formability are accounted for in this index. The advantages of using TFC over the FLC and other parameters of mechanical properties are evinced through a case study to compare the formability of the CR590DP and the CR980GEN3. Further, the strength and effectiveness of this new index in global formability evaluations are verified using a number of high strength steels. An explicit power law relationship is established between the TFC indices and experimental LDH results. The development and application of the TFC index promise a straightforward way to assess the overall global forming capacity of a material. It also serves as a more precise, yet simple tool for material comparisons and selections. Further development is ongoing to improve the accuracy of the index and remove undesirable assumptions.

Acknowledgment

The authors would like to thank United States Steel Corporation for the permission to publish the data in this paper.

Disclaimer

The material in this paper is intended for general information only. Any use of this material in relation to any specific application should be based on independent examination and verification of its unrestricted availability for such use and a determination of suitability for the application by professionally qualified personnel. No license under any patents or other proprietary interests is implied by the publication of this paper. Those making use of or relying upon the material assume all risks and liability arising from such use or reliance.

References

[1] Keeler S, Kimchi M and Mooney P H 2015 *Advanced High-Strength Steels Application Guidelines V5* (www.worldautosteel.org)

[2] Hu S J, Marciniak Z and Duncan J L 2008 *Mechanics of Sheet Metal Forming* (Butterworth-Heinemann)
[3] Keeler S 1988 Fifty Years of Sheet Metal Formability — Has Science Replaced the Art? *SAE Technical Paper* 880363
[4] Stören S and Rice J R 1975 Localized Necking in Thin Sheets *J. Mech. Phys. Solids* **23** pp 421-41
[5] Keeler S P and Brazier W G 1975 Relationship between Laboratory Material Characterization and Press Shop Formability *Proceedings of Microalloying* **75** pp 517-31
[6] Goodwin G 1968 Application of Strain Analysis to Sheet Metal Forming Problems in the Press Shop *SAE Technical Paper* 680093
[7] Raghavan K S, Van Kuren R C and Darlington H 1992 Recent progress in the development of forming limit curves for automotive sheet steels *SAE Technical Paper* 920437
[8] Abspoel M., Scholting M E and Droog J M 2013 A new method for predicting forming limit curves from mechanical properties *J. Mater. Process. Technol.* **213** pp 759-69
[9] Shi M 1995 Strain Hardening and Forming Limits of Automotive Steels *SAE Technical Paper* 950700
[10] Ghosh A K 1977 The influence of strain hardening and strain-rate sensitivity on sheet metal forming *J. Eng. Mater. Technol.* **99** pp 264-74
[11] Chen X, Niu C, Lian C, and Lin J 2017 The Evaluation of Formability of the 3rd Generation Advanced High Strength Steels QP980 based on Digital Image Correlation Method *Procedia Engineering* **207** pp 556-61
[12] Zhang L, Lin J, Min J, Ye Y, and Kang L 2016 Formability Evaluation of Sheet Metals Based on Global Strain Distribution *J. Mater. Eng. Perform.* **25** pp 2296-306
[13] Zeng D, Chappuis L, Xia Z C, and Zhu X 2008 A Path Independent Forming Limit Criterion for Sheet Metal Forming Simulations *SAE Technical Paper* 2008-01-1445
[14] ASTM International 2016 *Standard Test Methods for Tension Testing of Metallic Materials* E8/E8M
[15] ASTM International 2015 *Standard Test Method for Determining Forming Limit Curves* E2218-15
[16] Huang L and Shi M 2017 Determination of the Forming Limit Curve Using Digital Image Correlation-Comparison of Different Approaches to Pinpoint the Onset of Localized Necking *SAE Technical Paper* 2017-01-0301
[17] Huang L and Shi M 2018 Forming Limit Curves of Advanced High Strength Steels: Experimental Determination and Empirical Prediction *SAE Technical Paper* 2018-01-0804
[18] International Organization for Standardization 2008 *Metallic materials – sheet and strip – determination of forming-limit curves – part 2: Determination of forming-limit curves in the laboratory* 12004-02
[19] Min J, Stoughton T B, Carsley J E and Lin J 2016 Compensation for process-dependent effects in the determination of localized necking limits *Int. J. Mech. Sci.* **117** pp 115-34
[20] Wu W, Wang Y-W, Makrygiannis P, Zhu F, Thomas G A, Hector L G, Hu X, Sun X and Ren Y 2018 Deformation mode and strain path dependence of martensite phase transformation in a medium manganese TRIP steel *Mater. Sci. Eng. A* **711** pp 611-23